Homemade Micro-Raman Spectrometer and Design for Low-Wavenumber Spectral Measurement

Liu Kaishuo, Luo Xixi, Li Chun, Wang Qiyuan, Yang Jian*

Faculty of Energy Engineering, Yulin University, Yulin, 719000, China *Corresponding author

Abstract: Raman spectroscopy has been widely applied in fields such as materials science, biomedicine, and environmental monitoring. However, traditional Raman spectrometers suffer from high cost and limited measurement ranges. Due to the limitations of optical filters, most Raman spectrometers lack coverage in the low-wavenumber region (below 200 cm⁻¹). To address these issues, this project designs a homemade micro-Raman spectrometer based on 785 nm laser and proposes a conceptual design for a micro-Raman spectrometer that covers the low-wavenumber range.

Keywords: Raman Spectrometer, Optical Path System, Performance Improvement

1. Introduction

Raman spectroscopy is widely used across biology, chemistry, medicine, and physics due to its nondestructive nature and high chemical specificity^{[1]-[4]}. Particularly in the low-wavenumber region (<200 cm⁻¹), Raman signals can reveal key information such as lattice vibrational modes, intermolecular interactions, and phonon characteristics in crystalline materials, which is crucial for research on nanomaterials, two-dimensional materials, and soft matter systems. However, conventional commercial Raman spectrometers are constrained by high costs and technical limitations, leading to significant shortcomings in low-wavenumber measurements: first, inadequate optical filter performance results in poor Rayleigh scattering suppression, causing low-wavenumber signals to be overwhelmed by noise; second, existing systems have complex optical path designs that struggle to balance sensitivity and resolution, limiting their application in scenarios with strong fluorescence background or analysis of lowfrequency vibrational modes. To address these challenges, this study proposes a design for a homemade micro-Raman spectrometer based on 785 nm laser, aiming to overcome the limitations of narrow measurement range and excessive cost while providing a new solution for low-wavenumber detection. By optimizing the optical path system, the extraction efficiency and signal-to-noise ratio of lowwavenumber signals are significantly improved. Experimental results show that the modified spectrometer achieves a wide spectral coverage of 700-4500 cm⁻¹, with stable resolution in the lowwavenumber region at 3-4 cm⁻¹, and demonstrates superior performance in fluorescence background suppression and sensitivity compared to traditional instruments.

The significance of this study lies not only in validating the feasibility of a low-cost homemade Raman spectrometer but also in providing new insights for precise detection of low-frequency vibrational modes through innovative optical path design and filtering techniques. Subsequent research will further optimize the layout of optical components and the environmental control module to enhance system stability and expand its application potential in complex sample analysis.

2. Experimental Materials and Equipment

Olympus BX51 microscope (capable of independent high-precision microscopic imaging and serving as the core carrier for spectroscopic analysis); Invictus laser (as the excitation light source); high-performance optical components, including a dichroic mirror (Semrock, LPD02-785RU-25), lenses, objective lens, mirrors, laser cleaning filter (Semrock, LL01-785-25), and volume holographic filter (OptiGrate, BNF785); spectral analysis software (primarily for fluorescence background subtraction); and environmental control equipment.

ISSN 2706-655X Vol. 7, Issue 4: 1-5, DOI: 10.25236/IJFET.2025.070401

3. Experimental Principles

3.1 Optical System of the Raman Spectrometer

Currently, the most commonly used optical configuration in Raman spectrometer systems is the Czerny-Turner type (reflective) optical structure, consisting of an entrance slit, collimating mirror, grating, focusing mirror, and collection module^[5]. The Czerny-Turner optical structure can be divided into M type and crossed type; the M type exhibits relatively smaller coma aberration across the spectral measurement range, better resolution stability, and avoids secondary and multiple diffractions, while being easier to manufacture and align mechanically. Therefore, this paper adopts the M type Czerny-Turner optical structure for optical design^[6].

To improve detection sensitivity and extend the low-wavenumber detection range, we designed the optical path as shown in Figure 1. Figure 1(a) shows the schematic diagram of the Raman spectrometer optical path. The laser is emitted from a 785 nm continuous-wave laser, passes through a laser cleaning filter (Semrock, LL01-785-25), then through a dichroic mirror (Semrock, LPD02-785RU-25), and is focused onto the sample by the objective lens. The Raman scattering signal reflects off the objective lens, then reflects off the dichroic mirror, and subsequently reflects again, passing through two volume holographic filters (OptiGrate, BNF785), before coupling via a lens into the spectrometer (Ocean Optics, QE65pro). Figure 1(b) shows the laser (Invictus, INV-0104), Figure 1(c) shows the spectrometer, Figure 1(d) shows the self-made optical coupler, and Figure 1(e) shows the microscope (Olympus BX51).

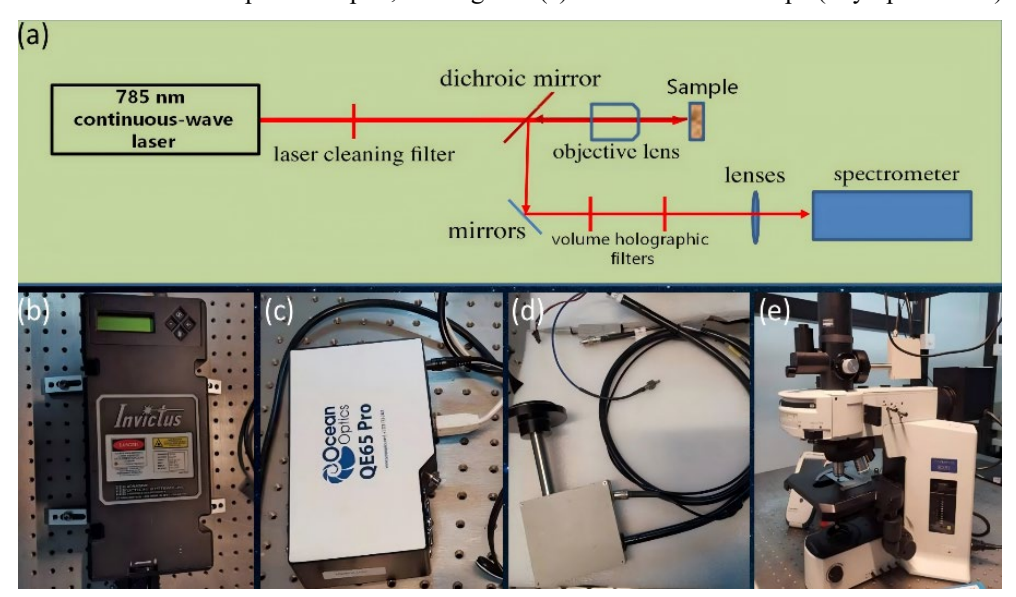


Figure 1 Schematic of the homemade Raman spectrometer optical path and corresponding component photographs.(a) Optical path diagram; (b) laser; (c) spectrometer; (d) optical coupler; (e) microscope system.

3.2 Optimization of Spectral Line Series

Due to insufficient performance of optical filters in low-frequency measurements, Rayleigh scattering suppression is poor, and low-wavenumber signals are easily overwhelmed by noise. Therefore, we optimize the optical path system by adopting a cascaded filtering structure combining ultra-filters with volume holographic filters, along with a fluorescence background subtraction algorithm, significantly improving the extraction efficiency and signal-to-noise ratio of low-wavenumber signals. The core optical path employs an M-type Czerny-Turner reflective design, integrated with Olympus BX51 microscope's UIS2 optical system and high-precision objectives, ensuring a balance between microscopic confocal performance and light throughput.

ISSN 2706-655X Vol. 7, Issue 4: 1-5, DOI: 10.25236/IJFET.2025.070401

4. Experimental Methods

4.1 Spectral Line Calibration

First, calibrate the spectrometer using a silicon wafer 520 cm⁻¹ peak (error <±1 cm⁻¹), and collect the spectrum of SERS substrate (without sample) as background. Focus the laser onto the sample surface, preview the signal (ensuring the 1660 cm⁻¹ peak is visible), then proceed with formal acquisition.

Based on the physical principles of Raman spectroscopy, laser from a 785nm continuous laser source passes through a laser cleaning filter, then through a dichroic mirror, and is focused onto the sample by the objective lens. The Raman scattered signal reflects back through the objective lens, is reflected by the dichroic mirror, then further reflected, passes through a volume holographic filter, and is coupled via a lens into the spectrometer. After every 5 samples, re-measure the GA₃ standard (1 mg/mL); if the peak position drifts by >2 cm⁻¹, recalibration is required.

4.2 Spectral line measurement

First, connect the power supply, turn on the microscope, and open the computer monitor connected to it; adjust the microscope for clear imaging. Then turn off the computer monitor, open the spectral imaging software, close the microscope, turn on the laser emitter, and adjust the laser wavelength. Set parameters in the software and run the system. Run for one week, then turn off the laser, restart for two weeks to obtain dark spectrum data, and save the data in document form. Then perform data processing. The actual optical path involves light emitted from an optical fiber coupling entering through a slit, being collimated by a concave mirror, incident upon a plane diffraction grating, where diffracted light is focused by a lens onto the CCD detector, producing a broadened diffraction spectrum that is finally detected. Finally, we use a peak identification algorithm on the obtained Raman spectrum from the detector to determine the positions and intensities of Raman peaks, which are used to determine molecular concentration and information.

5. Experimental Results and Error Analysis

5.1 Experimental Results

Due to the difficulty in accessing low-wavenumber measurement data, for data comparison purposes, we only present the Raman spectra obtained from the detector ranging from 700 cm⁻¹to 4500 cm⁻¹, as shown in Figure 2. The four spectral lines represent experimental data from a blossom inhibitor standard and gibberellin GA₃ standard (1 mg/mL), along with known Raman peak positions. The measurement range of the Raman spectrometer and the resolution test results are demonstrated to compare the resolution at different wavenumbers, typically around 3–4 cm⁻¹. During measurements, we also encountered fluorescence background interference; therefore, by optimizing the optical path system and adopting a cascaded filter structure using ultra-filter and volume holographic filters in combination with a fluorescence background subtraction algorithm, we eliminated the influence of fluorescence background on the data. We show the acquired fluorescence background spectrum in Figure 3(a) and the comparison of Raman spectra of Huping algae before and after fluorescence background subtraction in Figure 3(b).

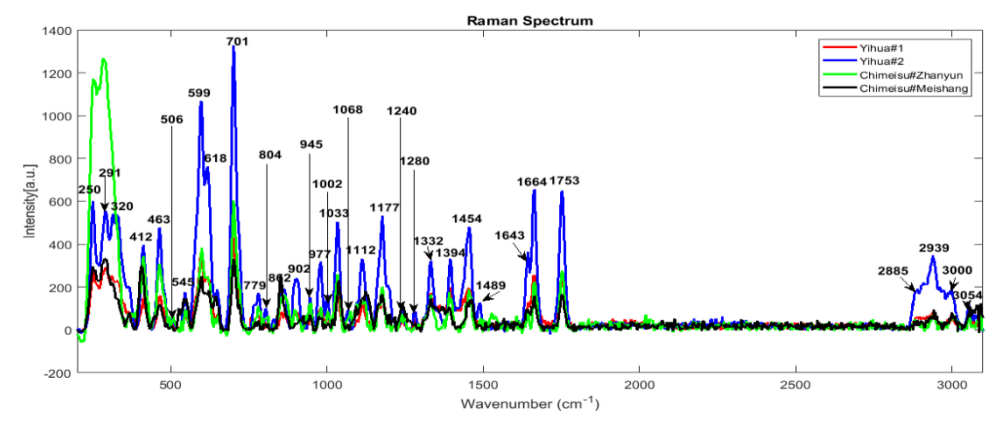


Figure 2 Raman spectra of standard flower suppressants and gibberellin AG₃

ISSN 2706-655X Vol. 7, Issue 4: 1-5, DOI: 10.25236/IJFET.2025.070401

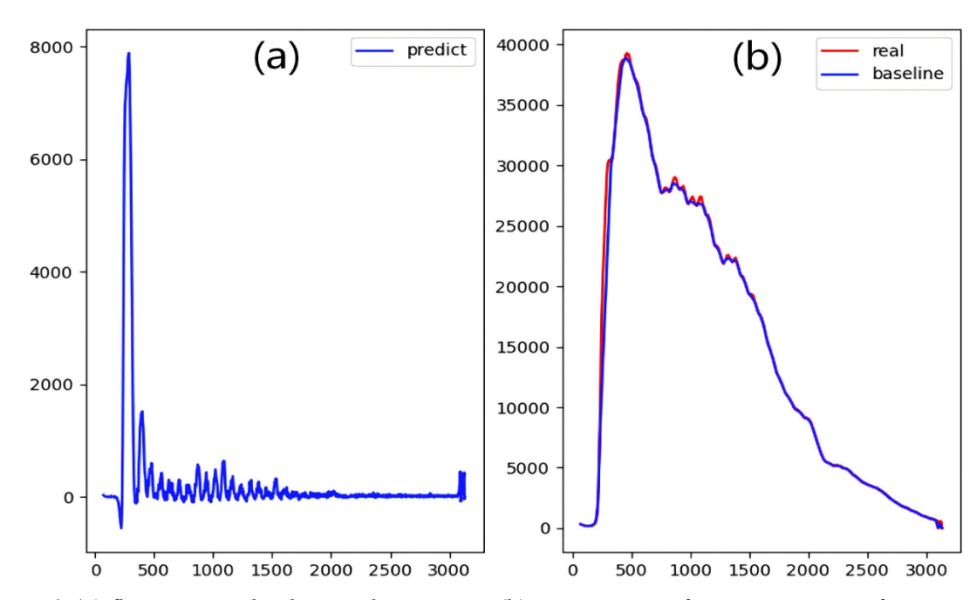


Figure 3 (a) fluorescence background spectrum; (b) comparison of Raman spectra of Huping algae before and after fluorescence background subtraction

Due to the impact of different optical components (such as filters and lenses) on spectrometer performance, the optical path core adopts a M type Czerny-Turner reflective structure. Combined with Olympus BX51 microscope's UIS2 optical system and high-precision objective lenses for sample measurement, we demonstrate the test results using standard samples (such as silicon wafers or solutions with known Raman peaks) and actual sample Raman spectra, comparing them with known data values. This method ensures a balance between microscopic confocal performance and light throughput. The experimental results ultimately indicate that the improved spectrometer achieves a wide spectral coverage of 700-4500 cm⁻¹ and maintains stable resolution at low wavenumbers at 3-4 cm⁻¹, while demonstrating superior performance over traditional devices in fluorescence suppression and sensitivity. Spectral measurement errors mainly originate from instrument limitations, environmental interference, and human factors: imperfections in optical components (such as non-uniform gratings, varying lens reflectivity, and misalignment) and mechanical vibrations affect system stability; fluctuations in light source power, wavelength drift, and detector non-linear response (including dark current noise) limit signal accuracy; spectral resolution is constrained by dispersive element performance, and sample inhomogeneity causes local measurement deviations. Changes in environmental temperature and humidity, as well as pressure fluctuations, cause drifts in optical parameters; wavelength calibration errors and data processing algorithms (such as baseline correction and peak fitting) may introduce systematic biases; meanwhile, operational mistakes during sample preparation and instrument use create additional error sources.

5.2 Error Analysis

Spectral measurement errors mainly originate from instrument performance limitations, environmental interference, and human factors: Imperfect optical components (such as non-uniform gratings, varying lens reflectivity, and alignment deviations) and mechanical vibrations affect system stability; fluctuations in light source power, wavelength drift, and detector nonlinear response (including dark current noise) limit signal accuracy; spectral resolution is constrained by the performance of dispersive elements, while sample inhomogeneity causes localized measurement bias. Variations in environmental temperature and humidity, as well as pressure fluctuations, can induce drifts in optical parameters; wavelength calibration errors and data processing algorithms (such as baseline correction and peak fitting) may introduce systematic biases, and operational mistakes during sample preparation and instrument use create additional error sources.

6. Experimental Conclusion

Using the designed optical path system, we successfully built a homemade Raman spectrometer, verifying the effectiveness of this design. For future improvements, we will start with optical components, aiming to extend the low-wavenumber measurement range by optimizing the selection and arrangement

International Journal of Frontiers in Engineering Technology

ISSN 2706-655X Vol. 7, Issue 4: 1-5, DOI: 10.25236/IJFET.2025.070401

of optical elements, thereby achieving better performance and results. Meanwhile, we will further optimize the environmental control module to enhance system stability and expand its application potential in complex sample analysis.

References

- [1] Xi X, Chongyang L. Perspective of Future SERS Clinical Application Based on Current Status of Raman Spectroscopy Clinical Trials[J]. Frontiers in Chemistry, 2021, 9665841.
- [2] Bo L ,Kunxiang L ,Xiaoqing Q , et al. Classification of deep-sea cold seep bacteria by transformer combined with Raman spectroscopy.[J]. Scientific reports, 2023, 13(1):3240.
- [3] Huirong H, Da-Wen S, Hongbin P, et al. Applications of Raman spectroscopic techniques for quality and safety evaluation of milk: A review of recent developments. [J]. Critical reviews in food science and nutrition, 2019, 59(5):770-793.
- [4] Shuangyan L, Ho S Y, Xinran F, et al. Understanding the lithium—sulfur battery redox reactions via operando confocal Raman microscopy[J]. Nature Communications, 2022, 13(1):4811.
- [5] Hui Z. Design and Analysis of High Resolution and Wide Spectral Range Micro Spectrometer[J]. Progress in Laser and Optoelectronics, 2020, 57(15): 275-281.
- [6] Wei B,Zhaoqing Y,Meng X, et al. Integrated design of ultra-high resolution spectrometer based on rotating grating[J].optical technique,2024,50(03):309-314.DOI:10.13741/j.cnki.11-1879/o4.2024.03. 008.